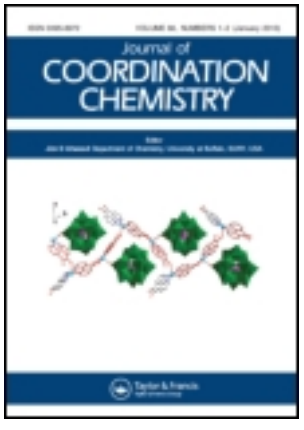

Journal of Coordination Chemistry
Publication details, including instructions for authors and subscription information:
http://www.tandfonline.com/loi/gcoo20

Chiral pyridinyloxazolidine ligands and copper chloride complexes

Sheryl L. Wiskur [a], Marc S. Maynor [a], Mark D. Smith [a], Cody I. Sheppard [a], Ravish K. Akhani [a], Perry J. Pellechia [a], Shae A. Vaughn [a] & Chengnien Shieh [a]

[a] Department of Chemistry and Biochemistry, University of South Carolina, Columbia, SC, USA

Accepted author version posted online: 14 Feb 2013.Published online: 27 Mar 2013.

To cite this article: Sheryl L. Wiskur, Marc S. Maynor, Mark D. Smith, Cody I. Sheppard, Ravish K. Akhani, Perry J. Pellechia, Shae A. Vaughn & Chengnien Shieh (2013) Chiral pyridinyloxazolidine ligands and copper chloride complexes, Journal of Coordination Chemistry, 66:7, 1166-1177, DOI: 10.1080/00958972.2013.775426

To link to this article: http://dx.doi.org/10.1080/00958972.2013.775426

Journal of Coordination Chemistry, 2013
http://dx.doi.org/10.1080/00958972.2013.775426

Chiral pyridinyloxazolidine ligands and copper chloride complexes

SHERYL L. WISKUR*, MARC S. MAYNOR, MARK D. SMITH, CODY I. SHEPPARD, RAVISH K. AKHANI, PERRY J. PELLECHIA, SHAE A. VAUGHN and CHENGNIEN SHIEH

Department of Chemistry and Biochemistry, University of South Carolina, Columbia, SC, USA

(*Received 24 May 2012; in final form 29 November 2012*)

Two chiral bidentate C1-symmetric 1,3-oxazolidine ligands (**1** and **2**) and coordination complexes with copper(II) chloride ($Cu_2Cl_4(C_{15}H_{14}N_2O)_2$ (**3**) and $[Cu_2Cl_4(C_{16}H_{16}N_2O)_2]\cdot CH_3OH$ (**4**)) were synthesized and characterized by X-ray crystallographic techniques. The ligands maintain the same stereochemistry within all structures, resulting in an *anti*-relationship between the 2,4-substituents. Structures **3** and **4** dimerized through bridging chlorides and **3** has an extended hydrogen bonding network resulting in an infinite 1D chain.

Keywords: Oxazolidine; Chiral ligands; Copper(II) chloride dimer

1. Introduction

The development of chiral coordination compounds often leads to unique topologies and has applications in catalysis and supramolecular chemistry [1–4]. One way to obtain chiral coordination compounds is through incorporation of chiral ligands. Oxazoline, a common core functionality found in many chiral ligands, is well studied and extensively used in asymmetric catalysis and supramolecular applications [5–9]. A less studied version of the oxazoline motif is the oxazolidine, which has the basic core structure of oxazoline but is fully saturated. Herein, we report the synthesis and structure of two new 1,3-oxazolidine ligands (**1** and **2**) that were subsequently incorporated into two copper coordination complexes, $Cu_2Cl_4(C_{15}H_{14}N_2O)_2$ (**3**) and $[Cu_2Cl_4(C_{16}H_{16}N_2O)_2]\cdot CH_3OH$ (**4**).

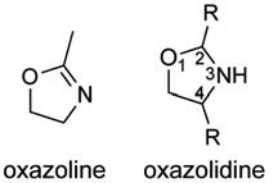

oxazoline oxazolidine

*Corresponding author. Email: wiskur@mailbox.sc.edu

Oxazolidine ligands have been employed more frequently as chiral auxiliaries [10] because of the ease of synthesis, but recently their use in catalysis has been demonstrated [11, 12]. For example, they have recently been used as ligands in a palladium-catalyzed allylation reaction [13], organozinc reactions [14, 15], and a palladium-catalyzed Diels–Alder reaction [16]. These ligands contain features that oxazolines do not, such as the presence of an additional stereocenter located adjacent to the metal- binding nitrogen as compared to the more planar oxazolines [11]. This brings a chiral center very close to the reaction center. Additionally, the oxazolidines have a different electronic structure due to an sp^3 hybridized nitrogen versus the sp^2 hybridized nitrogen found in oxazolines. Therefore, the development of new, chiral oxazolidine ligands and coordination compounds can expand and improve upon the field of asymmetric catalysis.

Two chiral bidentate C1-symmetric 1,3-oxazolidine ligands (**1** and **2**) were synthesized and coordinated to copper(II) chloride to form **3** and **4** (figure 1). Copper(II) chloride was chosen to show the coordination ability of the ligand, which consisted of two coordination sites, an oxazolidine nitrogen and a pyridine nitrogen. The oxazolidines were synthesized by condensation of an enantiomerically pure amino alcohol with either an aldehyde or a ketone (Scheme 1). The reaction proceeds through the formation of an imine, followed by nucleophilic attack of the alcohol to the imine to form the oxazolidine. Many oxazolidines derived from primary amines exist in equilibrium as a mixture of the imine intermediate and the closed product in solution (Scheme 1) [17, 18]. When the compound is in the oxazolidine form, two possible stereocenters can result from the alcohol attacking either face of the prochiral imine, adding to the complexity of possible products. In this article, the structures and synthesis of **1**–**4** will be discussed, highlighting the diastereomeric ratios of the ligands, the conformational differences of the ligands, and the details of coordination of the ligands to copper(II) chloride.

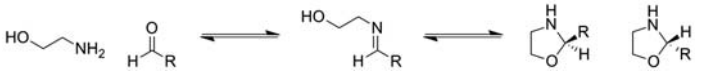

Scheme 1. Equilibrium of oxazolidine formation starting from an amino alcohol and an aldehyde resulting in two different oxazolidine stereoisomers.

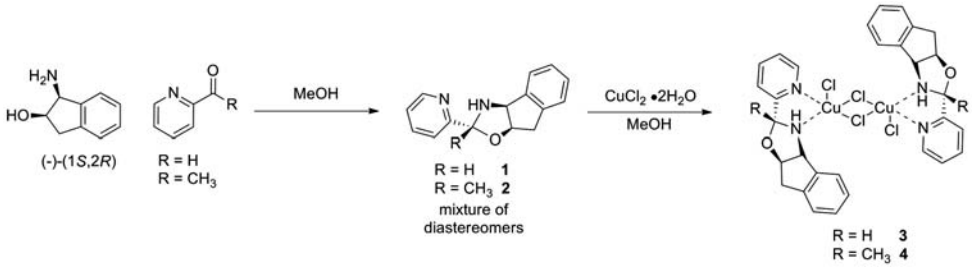

Figure 1. Synthetic route to ligands **1** and **2** and the copper coordination compounds **3** and **4**. (The orientation of the ligands to one another around the dimeric copper varies in structure **4** and is not drawn here as a definitive orientation.)

2. Experimental

2.1. *Materials*

2-Acetylpyridine (Aldrich, 99+%), (1*S*,2*R*)-*cis*-1-amino-2-indanol, 2-formylpyridine (Alfa Aesar, 99%), and $CuCl_2 \cdot 2H_2O$ (J.T. Baker) were used as obtained. ^1H NMR and ^{13}C NMR were obtained with a 300 MHz Varian spectrometer. UV–vis absorbance was collected using a Perkin-Elmer Lambda 35 UV–vis scanning spectrophotometer. Dry methanol was obtained by passing the previously degassed solvent through activated alumina columns.

2.2. *Synthesis of 1*

(1*S*,2*R*)-*cis*-1-Amino-2-indanol (0.5 g, 3.35 mmol) and 2-formylpyridine (0.36 g, 3.35 mmol) were stirred in 5 mL of dry methanol in a four dram vial. The solution was stirred at room temperature overnight. The solvent was removed by rotary evaporation and hexanes was added. The solvent was allowed to slowly evaporate to form a yellow oil and no further purification was done. The ^1H NMR showed a mixture of diastereomers in solution, not separable by column chromatography, but the conversion was quantitative by NMR (see Supplementary Material for ^1H and ^{13}C spectra of the crude mixture). HRMS (EI+) (M+) Calcd for ($C_{15}H_{14}N_2O^+$): 238.1100, observed: 238.1098.

2.3. *Synthesis of 2*

(1*S*,2*R*)-*cis*-1-Amino-2-indanol (0.5 g, 3.35 mmol) and acetyl pyridine (0.41 g, 3.35 mmol) were stirred in 5 mL of dry methanol in a four dram vial. The solution was stirred at room temperature overnight. The solvent was removed by rotary evaporation and the ^1H NMR showed a mixture of diastereomers and the open imine form in solution, not separable by column chromatography. The conversion to oxazolidine was 75% by NMR (see Supplementary Material for ^1H and ^{13}C spectra of the crude mixture). Hexanes was added and

Table 1. Crystal data and structure refinement for **2**, **3**, and **4**.

	2	**3**	**4**
Empirical formula	$C_{16}H_{16}N_2O$	$C_{30}H_{28}Cl_4Cu_2N_4O_2$	$C_{33}H_{36}Cl_4Cu_2N_4O_3$
Formula weight	252.31	745.44	805.54
Crystal system	Orthorhombic	Monoclinic	Triclinic
Space group	$P2_12_12_1$	$P2_1$	$P1$ (No. 1)
Unit cell dimensions			
a (Å)	5.6504(4)	7.6994(6)	9.1405(4)
b (Å)	11.3898(8)	11.0813(9)	10.1609(4)
c (Å)	19.9466(14)	17.6268(14)	27.3375(11)
α (°)	90	90	94.100(1)
β(°)	90	100.6910(10)	94.318(1)
γ (°)	90	90	90.567(1)
Volume (Å^3)	1283.70(16)	1477.8(2)	2525.01(18)
Z	4	2	3
Density (Calcd, Mg m^{-3})	1.305	1.675	1.589
Absolute coefficient (mm^{-1})	0.083	1.838	1.622
Final R indices ($I > 2\sigma$ (I))	$R1 = 0.0321$ $wR2 = 0.0715$	$R1 = 0.0357$ $wR2 = 0.0823$	$R1 = 0.0382$ $wR2 = 0.0819$

the solvent was allowed to slowly evaporate to form pale yellow needle crystallographic quality crystals. HRMS (EI+) (M+) Calcd for ($C_{16}H_{16}N_2O^+$): 252.1257, observed: 252.1257.

2.4. *Synthesis of 3*

Dry methanol (0.5 mL) was used to dissolve (15.3 mg, 0.09 mmol) $CuCl_2{\cdot}2H_2O$ in a one dram vial to form a blue-green solution. Ligand **1** (21.4 mg, 0.09 mmol) was dissolved in

Table 2. Selected bond lengths, bond angles, and torsional angles for **2**, **3**, and **4**.

Compound **2**	
Bond length (Å)	
C(6)–O(1)	1.429(2)
C(6)–N(2)	1.461(3)
N(2)–H(2N)	0.82(2)
C(6)–C(7)	1.511(3)
Bond angle (°)	
O(1)–C(6)–N(2)	103.79(15)
N(2)–C(6)–C(7)	112.22(16)
N(1)–C(5)–C(6)	115.55(16)
Torsional angle (°)	
N(1)–C(5)–C(6)–N(2)	−42.6(2)
Compound **3**	
Bond length (Å)	
Cu(1)–N(1)	2.037(3)
Cu(1)–N(2)	2.031(2)
Cu(1)–Cl(1)	2.2698(12)
Cu(1)–Cl(3)	2.6945(11)
Cu(2)–Cl(2)	2.9194(11)
C(6)–N(2)	1.470(5)
C(21)–N(4)	1.483(6)
Bond angle (°)	
N(2)–Cu(1)–N(1)	81.14(14)
N(2)–Cu(1)–Cl(1)	170.16(11)
N(2)–Cu(1)–Cl(2)	88.26(10)
Compound **4**	
Bond length (Å)	
Cu(1)–N(1)	1.992(3)
Cu(1)–N(2)	2.057(3)
Cu(1)–Cl(1)	2.3239(11)
Cu(1)–Cl(2)	2.2593(10)
Cu(1)–Cl(3)	2.6292(10)
Cu(2)–Cl(4)	2.2396(11)
Cu(2)–Cl(2)	3.1673(11)
Cu(2)–O(7)	2.629(3)
Cu(3)–Cl(5)	2.3389(10)
Cu(3)–Cl(7)	2.5400(10)
Cu(4)–Cl(6)	3.0723(11)
Cu(4)–O(8)	2.627(3)
Cu(6)–Cl(10)	2.7293(11)
Bond angle (°)	
N(1)–Cu(1)–N(2)	81.97(12)
N(3)–Cu(2)–N(4)	81.48(12)
N(5)–Cu(3)–N(6)	81.75(12)
N(7)–Cu(4)–N(8)	82.03(12)
N(9)–Cu(5)–N(10)	81.74(12)
N(11)–Cu(6)–N(12)	81.87(12)

1 mL of dry methanol in an NMR tube. The $CuCl_2 \cdot 2H_2O$ solution was slowly added to the ligand solution resulting in two layers. The tube was allowed to sit overnight at room temperature undisturbed. Dark blue bar crystals were obtained.

2.5. *Synthesis of 4*

Dry methanol (0.5 mL) was used to dissolve (20.7 mg, 0.12 mmol) $CuCl_2 \cdot 2H_2O$ in a one dram vial to form a blue-green solution. Ligand **2** (30.6 mg, 0.12 mmol) was dissolved in 1 mL of dry methanol in an NMR tube. The $CuCl_2 \cdot 2H_2O$ solution was slowly added to the ligand solution resulting in two layers. The mixture was allowed to sit overnight at room temperature undisturbed. Green plate-shaped crystals were obtained.

2.6. *X-ray crystallography*

X-ray diffraction intensity data for **2**–**4** were measured at 150(2) K on a Bruker SMART APEX diffractometer (Mo Kα radiation, $\lambda = 0.71073$ Å) [19]. The raw area detector data frames were processed with SAINT+ [19]. The reported unit cell parameters were determined by least-squares refinement of 3360 reflections (**2**), 7020 reflections (**3**), and 7925 reflections (**4**) from the data sets. Direct methods structure solution, difference Fourier calculations, and full-matrix least-squares refinement against F^2 were performed with SHELXTL [20]. Further information regarding data collection and structure solution is found in table 1 and in Supplementary Material. Selected bond lengths and angles are found in table 2.

3. Results and discussion

3.1. *Synthesis of 1 and 2*

Pyridinyloxazolidines **1** and **2** were synthesized from condensation of enantiomerically pure (1*S*,2*R*)-*cis*-1-amino-2-indanol and 2-formylpyridine or 2-acetylpyridine, respectively. The reaction proceeds through the formation of an imine intermediate from the reaction between the amine and the aldehyde or ketone. The oxazolidine ring forms when the alcohol acts as a nucleophile toward the imine closing the cycle. In solution, these open and closed forms are in equilibrium with each other [17,18]. In this article, a rigid amino alcohol was chosen to force the equilibrium toward oxazolidine product formation. The ^{1}H NMR shows complete conversion of 2-formylpyridine to **1** and 75% conversion of 2-acetylpyridine to **2** with the remaining 25% of material as the imine (see Supplementary Material). Our oxazolidine yield is higher than similar systems in the literature, presumably due to the preorganized amino alcohol [18]. Once the ring is formed, the oxazolidine product has an additional stereocenter, resulting in the possibility of two different diastereomeric products. Ultimately, **1** and **2** were obtained as a mixture of diastereomers in solution. The ^{1}H NMR spectra of **1** and **2** showed the presence of both diastereomers in a ratio of 1 : 6.4 for **1** and 1 : 1.7 for **2** (see Supplementary Material). NOESY experiments revealed the structure of the major diastereomer of **1** and **2** as the structures presented in figure 1 (see Supplementary Material). Interestingly, the structure of **2** was also elucidated using single crystal X-ray diffraction from a crystal that contained only one of the possible

diastereomers. X-ray quality crystals of all three crystal structures discussed below (**2**–**4**) contained the same oxazolidine diastereomer.

3.2. *Structural characterization of 2*

The crystal structure of the major diastereomer of **2** (figure 2) was obtained upon slow evaporation of hexanes from the mixture of diastereomers and crystallized in a chiral space group as an enantiomerically pure crystal and a single diastereomer. Since the absolute configurations at C(16) and C(8) were *S* and *R*, respectively, the stereochemistry at C(6) was determined to be *R* configuration. This places the substituents in the 2,4-positions on the 1,3-oxazolidine ring in an *anti*- relationship (pyridyl substituent and aryl substituent on C(16)). This is consistent with other reported structures derived from *cis*-1-amino-2-indanol [21]. When other amino alcohols are employed, it is more common to observe a *cis* relationship between the 2,4-position substituents on 1,3-oxazolidines [10].

This *anti*-orientation between the substituents is maintained in all the structures reported herein. The crystal structure of **2** also shows the five-membered oxazolidine ring adopts an envelope conformation with O(1)–C(8)–C(16)–N(2) in a semi-planar conformation with a torsion angle of only −5.64(18)°. The final atom in the cycle, C(6), is bent out of the plane with a torsion angle of 27.33(18)° for C(16)–C(8)–O(1)–C(6). An interesting feature of **2** is the presence of hydrogen on N(2) [14, 21], since a majority of oxazolidines are derived from substituted amines. The newly formed C(6)–O(1) and C(6)–N(2) bonds had bond lengths of 1.429(2) and 1.461(3) Å and an O(1)–C(6)–N(2) bond angle of 103.79 (15)° for the tetrahedral carbon, which are similar to other oxazolidines in the literature [21–23].

3.3. *Structural characterization of 3*

Compound **3** (figure 3) crystallized in the monoclinic space group $P2_1$ as enantiopure blue bar-shaped crystals. The unit cell of **3** shows two conformationally independent versions of the oxazolidine ligand **1** complexed with a copper(II) chloride, which dimerizes through bridging chloride anions. The bicyclic, bidentate ligand chelates the copper cation through

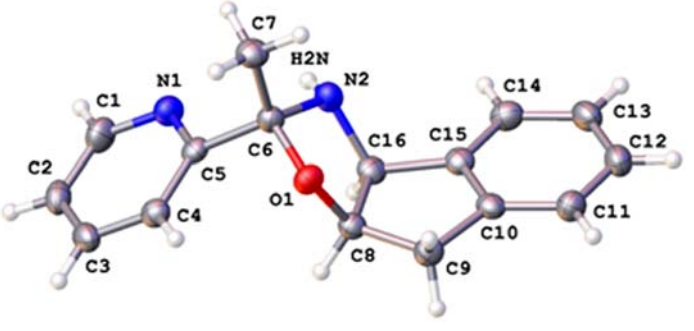

Figure 2. Crystal structure of **2**. Displacement ellipsoids drawn at the 50% probability level. Due to lack of heavy atoms in the crystal the stereochemistry cannot be determined directly from the X-ray data, but the conformation at C6 (*R*) was determined from the stereocenters C8 (*R*) and C16 (*S*) set from synthetic information.

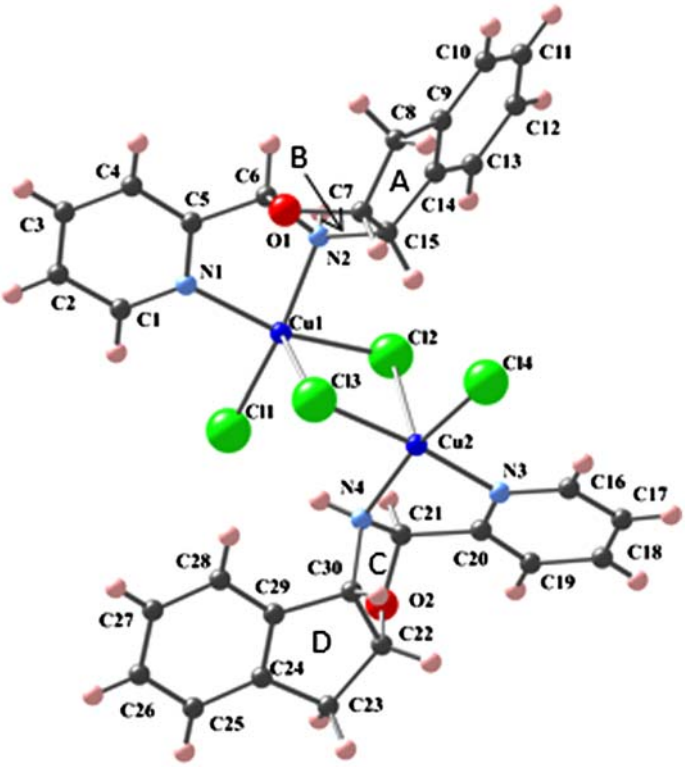

Figure 3. X-ray crystal structure of the asymmetric unit of **3**, shown as a ball and stick model. Fused five-membered rings labeled A–D.

two nitrogen atoms, an sp^2 pyridine nitrogen and a secondary sp^3 oxazolidine nitrogen. The distorted square pyramidal copper cations have a coordination sphere consisting of two bridging chloride anions, one terminal chloride anion, and two neutral nitrogen donors from the chelation of **1**. Each copper has a bridging chloride in the axial position with bond lengths of 2.6945(11) Å and 2.9194(11) Å for $Cu(1)–Cl(3)_{ax}$ and $Cu(2)–Cl(2)_{ax}$, respectively, where one of the bonds is longer than the other. The rest of the ligands are found in the equatorial positions. The copper–copper distance is 3.5850(7) Å, similar to other copper(II) chloride systems [24–26]. Bond angles around the coordinated copper cations deviate from the optimal 90° by a range of 5–10°. The observed distortion is likely due to the limited flexibility between the two coordinating nitrogens of the ligand.

The two ligands in the asymmetric unit of **3** are the same diastereomer, with minor conformational differences throughout the ligands. The stereocenters of both ligands maintain the same *R* and *S* configuration at each center relative to each other. There is also an *anti*-relationship between the substituents on the 1,3-oxazolidine rings, specifically relating the 2,4-substituents C(6) and C(15), as well as C(21) and C(30). This is the same relationship as seen above in **2**.

Ligand **1** contains two fused five-membered rings, and upon coordination to copper, conformational variations between the two ligands found in the asymmetric unit arise within these rings. Ring A, shown in figure 3, was found to be relatively planar, while the

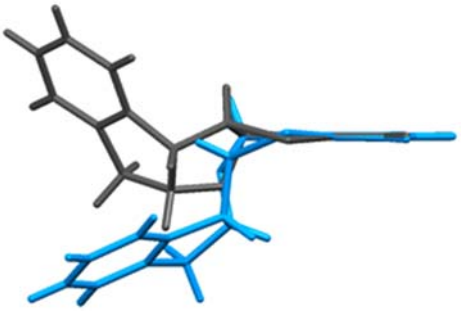

Figure 4. Comparison of the conformations of the two crystallographically independent ligands of **3**. Pyridyl rings superimposed. Gray = Ligand N(1)/N(2)/O(1), etc., coordinated to Cu(1). Blue = Ligand N(3)/N(4)/O(2), etc., coordinated to Cu(2) (http://dx.doi.org/10.1080/00958972.2013.775426 for color version).

complementary ring D is found in an envelope conformation with C(22) out of the plane of the ring with a conformational angle of 15.2(5)°. The five-membered oxazolidine rings B and C (figure 3) are complementary between the two ligands, but are in different conformations. Both are in envelope conformations with a different atom out of the plane of the other atoms. The newly formed tetrahedral carbon C(6) is out of the plane in ring B and the oxazolidine oxygen O(2) in ring C is out of the plane. There is also variation in the five-membered rings formed between the ligands and the copper cations. The atoms around Cu(1) are relatively planar in relationship to each other with N(2) out of plane, while the atoms around Cu(2) are highly twisted throughout. Figure 4 shows the two ligands superimposed on each other with the pyridines lined up, highlighting these conformational differences between the two ligands. The gray ligand contains rings A and B and the blue ligand contains rings C and D.

Coordination compound **3** also formed an extended tertiary structure due to the presence of the hydrogens on the oxazolidine nitrogens, N(2)H and N(4)H. The extended structure is the result of intra- and intermolecular hydrogen bonding to the monodentate chlorides and a difference between the ligands orientation or relationship to each other coordinated to the metal. The nitrogens are both set in the *R* configuration but they are bound to the copper dimer in a head to tail fashion, which results in one of the N–H hydrogens N(4) pointing into the center of the complex to obtain the internal hydrogen bond and the other N–H hydrogen N(2) pointing externally and connects to the adjacent complex to form the intermolecular hydrogen bond. This hydrogen bonding pattern creates an infinite 1D chain along the crystallographic *a*-axis (figure 5).

3.4. *Structural characterization of 4*

Compound **4** (figure 6), which consists of **2** chelated to copper(II) chloride, crystallized in the triclinic space group *P*1 (No. 1) as green plate crystals that are enantiopure. The asymmetric unit of **4** is quite different than the asymmetric unit observed for **3** due to the additional methyl group on the oxazolidine ring. The unit cell is much more complex and contains three independent $Cu_2Cl_4(C_{16}H_{16}N_2O)_2$ complexes, with two methanol molecules loosely coordinated and one methanol uncoordinated. All of the copper cations have a coordination sphere consisting of two bridging chlorides, but there are six unique copper

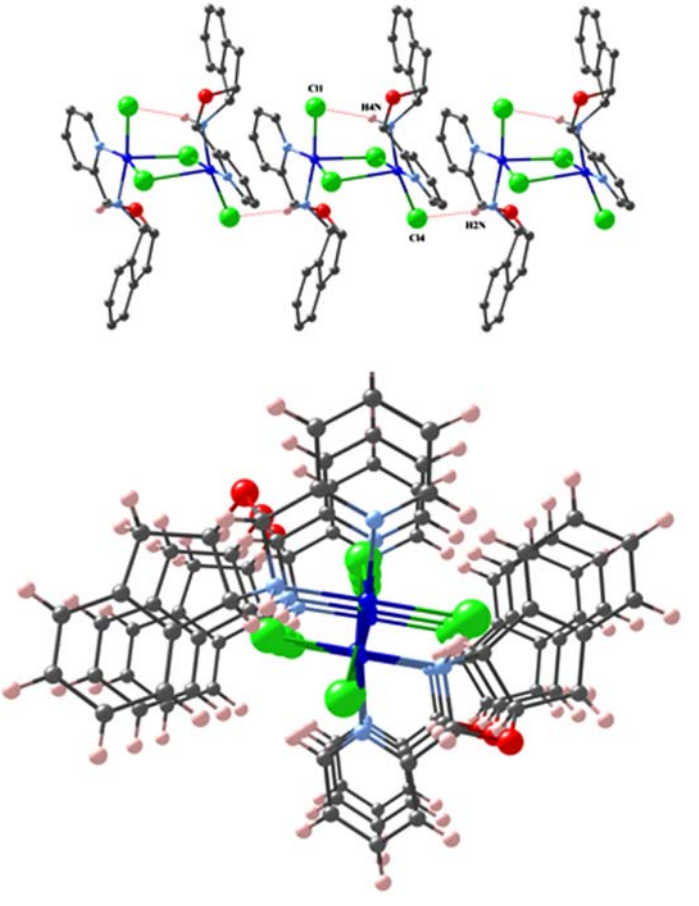

Figure 5. Top: 1-D chain formed by **3** via intra- and intermolecular NH···Cl hydrogen bonds (red dashed lines) viewed along the *b*-axis. Bottom: View along the *a*-axis, looking down the copper centers of the 1-D chain of **3**. (http://dx.doi.org/10.1080/00958972.2013.775426 for color version)

environments, in which two coppers display distorted square pyramidal geometry Cu(5) and Cu(6), two coppers have irregular trigonal pyramidal geometry Cu(1) and Cu(3), and two coppers have an elongated octahedral geometry Cu(2) and Cu(4). The octahedral coppers have loosely coordinated methanols as the sixth ligands and elongated Cu-bridged chloride bonds (3.1673(11) and 3.0723(11) Å) [26]. Axial ligands on both consist of coordinated methanol and bridging chloride. Similar to structure **3**, the axial ligands on the square pyramidal coppers are bridging chlorides. When the copper is trigonal pyramidal, the axial ligands are pyridine nitrogen and one bridging chloride. The copper–copper distances range between 3.5805(6) and 3.7571(6) Å, again consistent with other structures containing chloride bridging coppers [24–26].

All of the stereocenters in the six conformationally different ligands contain the same configuration at each center, which are the same absolute configurations found in **2** and **3**. This again results in an *anti*-substitution of the 2,4-substituents, specifically the 2-pyridyl and the aryl substituent. All of the bidentate ligands still coordinate the copper through

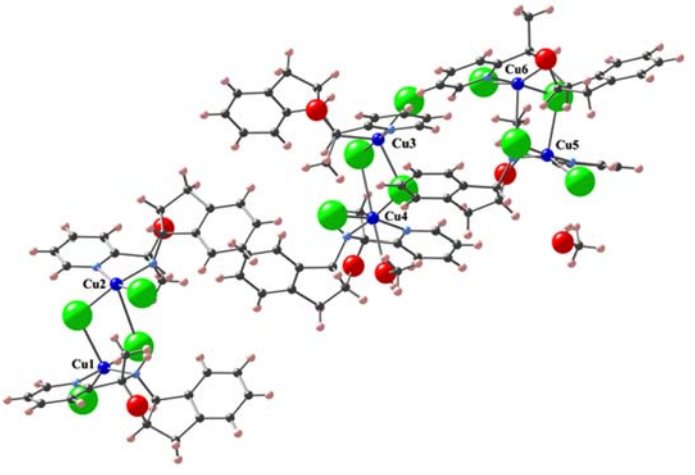

Figure 6. Asymmetric unit of **4**, which consists of six distinct copper environments and six conformationally distinct ligands.

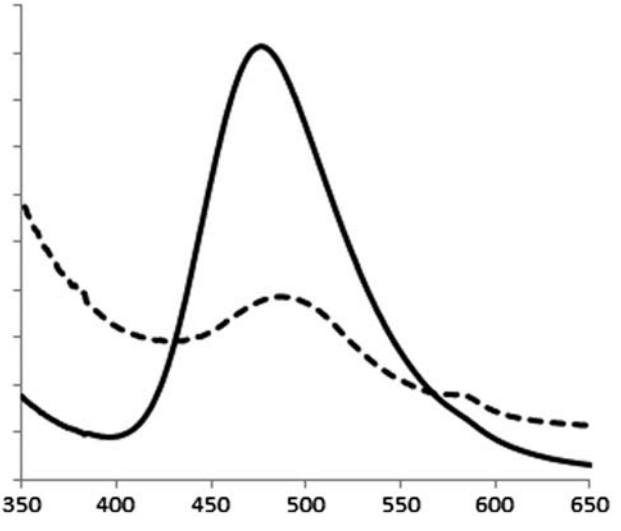

Figure 7. The normalized UV–vis absorbance of **3** (solid line) and **4** (dashed line).

the pyridine and the oxazolidine nitrogens, and two ligands bind per copper dimer. The relationship of the ligands to each other varies throughout the structure. In two of the copper dimers, the two ligands bind in a head to head orientation, while in the third copper dimer the ligands are in a head to tail orientation, similar to the orientation found in **3**. Finally, each of the Cu1/Cu2 and Cu3/Cu4 and Cu5/Cu6 forms 1D chains along the *b*-axis with symmetry-equivalent complexes via OH···Cl hydrogen bonding, and in the case of Cu5/Cu6, NH···O hydrogen bonding also (see Supplementary Material).

3.5. *Absorption properties*

The UV–vis absorbances of **3** and **4** were taken in the solid state between 200 and 800 nm (figure 7, 350–650 nm normalized). Both coordination compounds had intense absorbance below 400 nm (not shown) that is presumably attributed to absorbance of the coordinated ligands. Compound **3** had an additional broad absorbance band with a λ_{max} of 475 nm and **4** had a similar broad absorbance band with a λ_{max} of 487 nm and an additional small band near 590 nm. The longer wavelength absorbance may correspond to the ligand to metal charge transfer band [27].

4. Conclusions

The synthesis and characterization of two new chiral oxazolidine ligands and their coordination with copper(II) chloride are highlighted. The ligands are synthesized from enantiomerically pure *cis*-1,2-aminoindanol and an aldehyde or ketone, and only one of the two possible diastereomers crystallized. The ligands differ by the presence of one additional methyl group, and even though the ligands maintain the same stereochemistry throughout, the asymmetric unit of copper dimerized structures of **3** and **4** differ dramatically. These structures are a result of differences in ligand conformations, copper coordination spheres, and ligand–ligand orientations. Since **3** is derived from a primary amine, there is an NH hydrogen available for hydrogen bonding, with results in an infinite 1D chain, and has a simpler asymmetric unit than **4**. We are currently exploring the use of these ligands in catalysis due to the unusual *anti*-orientation of the 2,4-substituents and the synthesis of other new oxazolidine derived ligands.

Supplementary material

^{1}H and ^{13}C NMR spectra and additional information regarding X-ray crystal data collection can be found in the Supplementary Material. Full cif files reside with the Cambridge Crystallographic Data Center, 883718 for **2**, 883719 for **3**, and 883720 for **4**. Copies of the data can be obtained, free of charge, on application from CCDC, 12 Union Road, Cambridge CB2 1EZ, UK (Fax: +44 1223 336033 or E-mail: deposit@ccdc.cam.ac.uk).

Acknowledgements

We gratefully acknowledge support from startup funds from the University of South Carolina and the National Science Foundation CAREER Award CHE-1055616. We would also like to thank Professor Hanno zur Loye for helpful discussions.

References

[1] M.G. Finn. *Chirality*, **14**, 534 (2002).
[2] T.J. Wenzel, J.D. Wilcox. *Chirality*, **15**, 256 (2003).
[3] L. Pu. *Chem Rev.*, **104**, 1687 (2004).

[4] J. Crassous. *Chem. Soc. Rev.*, **38**, 830 (2009).
[5] G. Desimoni, G. Faita, K.A. Jørgensen. *Chem. Rev.*, **111**, PR284 (2011).
[6] F. Riobé, N. Avarvari. *Coord. Chem. Rev.*, **254**, 1523 (2010).
[7] H.-J. Kim, Y.-H. Kim, J.-I. Hong. *Tetrahedron Lett.*, **42**, 5049 (2001).
[8] S.-G. Kim, K.-H. Kim, J. Jung, S.K. Shin, K.H. Ahn. *J. Am. Chem. Soc.*, **124**, 591 (2002).
[9] S.-G. Kim, K.-H. Kim, Y.K. Kim, S.K. Shin, K.H. Ahn. *J. Am. Chem. Soc.*, **125**, 13819 (2003).
[10] C. Agami, F. Couty. *Eur. J. Org. Chem.*, **677**, (2004).
[11] C.A. Caputo, N.D. Jones. *Dalton Trans.*, 4627 (2007).
[12] C. Wolf, H. Xu. *Chem. Commun.*, **47**, 3339 (2011).
[13] A.L. Braga, C.C. Silveira, M.W.G. de Bolster, H.S. Schrekker, L.A. Wessjohann, P.H. Schneider. *J. Mol. Catal. A: Chem.*, **239**, 235 (2005).
[14] C. Wolf, S. Liu. *J. Am. Chem. Soc.*, **128**, 10996 (2006).
[15] R.W. Parrott II, S.R. Hitchcock. *Tetrahedron: Asymmetry*, **18**, 377 (2007).
[16] H. Nakano, K. Takahashi, Y. Okuyama, C. Senoo, N. Tsugawa, Y. Suzuki, et al. *J. Org. Chem.*, **69**, 7092 (2004).
[17] F. Fülöp, K. Pihlaja, K. Neuvonen, G. Bernáth, G. Argay, A. Kálmán. *J. Org. Chem.*, **58**, 1967 (1993).
[18] M. Juhász, L. Lázár, F. Fülöp. *Tetrahedron: Asymmetry*, **22**, 2012 (2011).
[19] Bruker Analytical X-ray Systems, Inc., Madison, Wisconsin (2001).
[20] G.M. Sheldrick, Bruker Analytical X-ray Systems, Inc., Madison, Wisconsin (2000).
[21] Z. Xu, J. Mao, Y. Zhang. *Org. Biomol. Chem.*, **6**, 1288 (2008).
[22] S.A. Cardile, M.C. Jennings, N.D. Jones. *Dalton Trans.,* 4672 (2006).
[23] B.A. Shainyan, M.V. Ustinov, V.K. Bel'skii, L.O. Nindakova. *Russ. J. Org. Chem.*, **38**, 104 (2002).
[24] E. Colacio, M. Ghazi, R. Kivekäs, J.M. Moreno. *Inorg. Chem.*, **39**, 2882 (2000).
[25] C.J. O'Connor, E.E. Eduok, J.W. Owens, E.D. Stevens. *Inorg. Chim. Acta*, **117**, 175 (1986).
[26] K. Butsch, A. Klein, M. Bauer. *Inorg. Chim. Acta*, **374**, 350 (2011).
[27] S.-L. Ma, X.-X. Sun, S. Gao, C.-M. Qi, H.-B. Huang, W.-X. Zhu. *Eur. J. Inorg. Chem.*, **846**, (2007).